

Course II: Compact Objects, the Dynamic Radio Sky, and 21st Century Radio Telescope Facilities

Jim Cordes
Professor of Astronomy
Cornell University

Five Lectures:

1. Astrophysics of neutron stars and other compact objects
2. Pulsar astrophysics (continued), plasma propagation effects on pulsar surveys and timing
3. Precision imaging and astrometry
4. The dynamic radio sky (transients and variability)
5. New radio telescope arrays for key science and discovery



Cornell University

9/13/11

Course II: Compact Objects, the Dynamic Sky and 21st Century Radio Telescopes

1

Pulsar Populations: $P - \dot{P}$ Diagram

• Magnetars+high-field pulsars

- $P \sim 5-12$ s
- $B \sim 10^{14} - 10^{15}$ G

• Canonical pulsars

- $P \sim 20\text{ms} - 5\text{s}$
- $B \sim 10^{12 \pm 1}$ G

• Recycled/Millisecond pulsars (NS-NS binaries, MSPs)

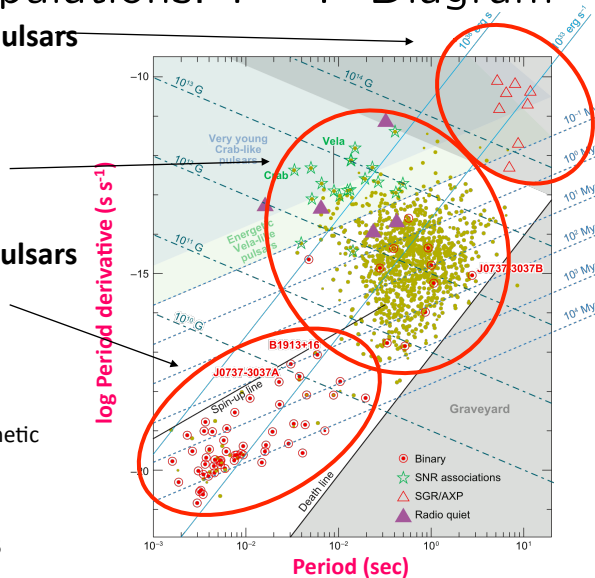
- $P \sim 1.4 - 20\text{ms}$
- $B \sim 10^8 - 10^9$ G

• Braking index n :

- $\dot{P} \propto P^{2-n}$, $n=3$ magnetic dipole radiation

• Death line

• Strong selection effects



12 Sep '11

Course II: Compact Objects, the Dynamic Sky and
21st Century Radio Telescopes

2

Where is the action?

- Sub-hour NS-NS binaries, NS-BH binaries
- Sub-millisecond pulsars --- or not --- providing constraints on EoS, gravitational wave emission, mountains on NS
- Many NS mass measurements: constraints on EoS
- Extragalactic pulsars and magnetars
 - requires SKA sensitivity for periodic sources
 - Giant pulses: Arecibo to $\sim 1\text{-}5$ Mpc SKA to Virgo cluster
- Better understanding of magnetospheric physics through combined Fermi detections of pulsars and radio beaming studies
- Discovery of many new, strange, fast transient sources
 - mostly neutron star variants or something else?
 - prompt radio bursts from GRBs (short bursts most likely)
- Pulsars orbiting Sgr A* + constraints of space time around a $4 \times 10^6 M_{\odot}$ black hole
- Strong constraints on/detection of nano-Hertz gravitational waves and constraints on massive-black hole astrophysics, cosmic strings

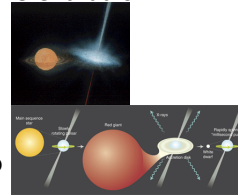
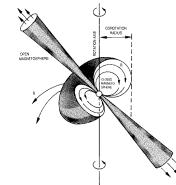
12 Sep '11

Course II: Compact Objects, the Dynamic Sky and 21st Century Radio Telescopes

3

Manifestations of NS:

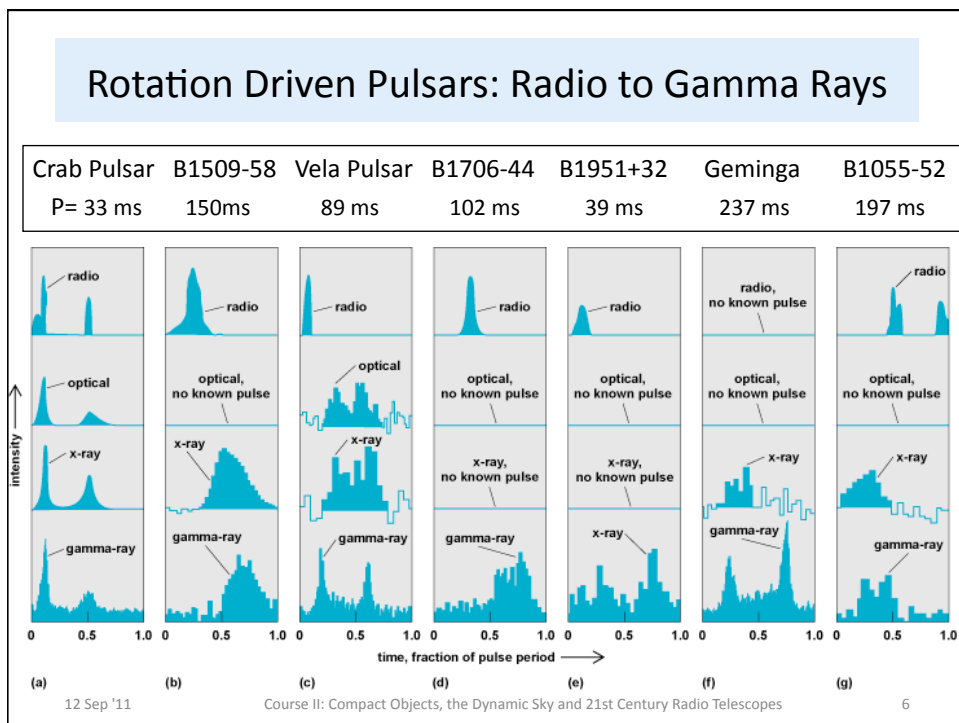
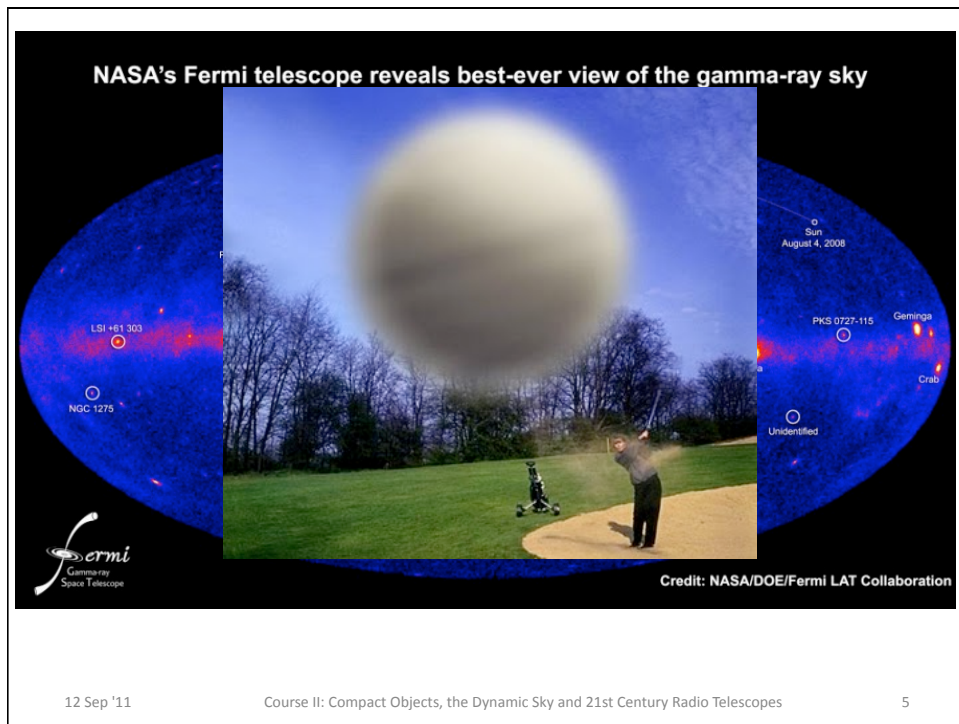
- Rotation driven:
 - “radio” pulsars (radio $\rightarrow \gamma$ rays)
 - magnetic torque $\dot{E} \propto I\Omega\dot{\Omega} \propto IB^2\Omega^4$
 - incoherent, nonthermal radiation (optical \rightarrow gamma rays)
 - $\gamma\gamma \rightarrow e^+e^-$ + plasma instability \Rightarrow coherent radio
- Accretion driven:
 - X-rays $L_x = \epsilon\dot{M}c^2$
 - LMXB, HMXB
- Magnetic driven: Crustquakes?
 - Magnetars (AXPs, SGRs) $L_x \gg \dot{E}$ $L_x \propto \frac{d}{dt}B^2$
 - Spindown from very high magnetic fields ($> 10^{14}$ G)
- Gravitational catastrophes
 - Subclass of Gamma-ray bursts (NS-NS or NS-BH inspiral)?



12 Sep '11

Course II: Compact Objects, the Dynamic Sky and 21st Century Radio Telescopes

4



THE ASTROPHYSICAL JOURNAL, 196:51-72, 1975 February 15
© 1975. The American Astronomical Society. All rights reserved. Printed in U.S.A.

THEORY OF PULSARS: POLAR GAPS, SPARKS, AND COHERENT MICROWAVE RADIATION

M. A. RUDERMAN*

AND

P. G. SUTHERLAND†

Department of Physics, Columbia University

Received 1974 April 29; revised 1974 July 8

ABSTRACT

The huge magnetic fields characteristic of pulsars cause the nuclei (largely iron) of the stellar surface to form a tightly bound condensed state. Except for the very young Crab pulsar, theory and observation both support the view that the stellar surface is not hot enough to sustain an outflow of positive ions to balance the outflow of electrons as charge leaves the magnetosphere through the light cylinder along the open magnetic field lines. Adopting the conventional assumption that electrons do not return to the neutron star by coming back through the light cylinder along the open field lines, we are led to the following consequences for a neutron star whose magnetic moment tends to be antiparallel (as opposed to parallel) to its spin angular momentum: A polar magnetospheric gap is formed that spans the open field lines from the stellar surface up to an altitude of about 10^8 cm. In the gap $\mathbf{E} \cdot \mathbf{B} \neq 0$, although it vanishes essentially everywhere else in the near magnetosphere. The potential difference between the base and top of the gap is about 10^8 volts. The gap continually breaks down (sparking) by forming electron-positron pairs on a time scale of a few microseconds. The gap positrons move out along the open field lines, and electrons flow to the stellar surface to close the pulsar's homopolar generator circuit as in the related Sturrock model.

We show how this can lead to injection into the near magnetosphere of ultrarelativistic positrons and the pairs subsequently produced by curvature radiation from the positrons leads to coherent microwave radiation in the frequency range and with remarkably many of the characteristics observed in pulsars. The properties and energetics of the sparking in the gap lead directly to (i) the maximum total luminosity of the pulsar and its dependence on period P : $L_{\text{max}} \sim 10^{40} P^{-1/2}$ ergs s^{-1} ; (ii) the observed drifting of subpulses and quantitative expressions for P_2 and P_3 (assuming that the sparking is localized, rapidly fluctuating but only rarely self-quenching); (iii) microstructure of pulses; (iv) the turnover of a pulsar as its period increases, and (v) apparent weakening of the magnetic field in older pulsars. The production of coherent microwave radiation in the near magnetosphere results in substantial qualitative agreement with observations in these areas: (i) shapes and widths of pulse envelopes, (ii) their period and frequency dependence, and (iii) the sweep of linear polarization through the pulse envelope.

Subject heading: pulsars

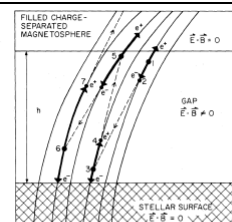


FIG. 3.—Breakdown of the polar gap. The solid lines are polar field lines of average radius of curvature ρ ; for a pure dipole field $\rho \sim (Rc/2)^{1/2} \sim 10^8 P^{1/2}$ cm, but for a realistic pulsar one expects $\rho \sim 10^8$ cm if many multipoles contribute near the surface. A photon (of energy $> 2mc^2$) produces an electron-positron pair at 1. The electric field of the gap accelerates the positron out of the gap and accelerates the electron toward the stellar surface. The electron moves along a curved field line and radiates an energetic photon at 2 which goes on to produce a pair at 3 once it has a sufficient component of its momentum perpendicular to the magnetic field. This cascade of pair production—acceleration of electrons and positrons along curved field lines—curvature radiation—pair production results in a “spark” breakdown of the gap.

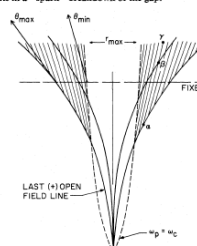


FIG. 8.—The region of coherent microwave radiation. Electrons and positrons move out along the open magnetic field lines. The bunching instability of frequency ω_0 (as defined in the text) excited by the primary positrons is strongly coupled to curvature radiation outside the dashed line $\omega = \omega_0$; the bunching may persist out to ρ_{max} . Radiation of frequency ω is produced at a distance from the star given by eq. (64): $\omega \approx \omega_0 r^{1/2}$. The straight lines pointing toward the pulsar star are the loci of constant tangent (to the magnetic field) direction. Thus, electrons and positrons at the points a, b, c radiate in the same direction but at respectively lower frequencies.

12 Sep '11

Course II: Compact Objects, the Dynamic Sky and 21st Century Radio Telescopes

Mind the Gaps

- Basics of magnetospheres
 - Goldreich & Julian (1969)
- Polar cap gaps for canonical pulsars
 - Sturrock (1970)
 - Ruderman & Sutherland (1975)
- Outer gaps for energetic young pulsars
 - Cheng and Ruderman
- Slot gaps
 - Arons et al. late 1970's
- basic explanation of P-Pdot diagram
- Some understanding of radio and high-energy beaming, energetics

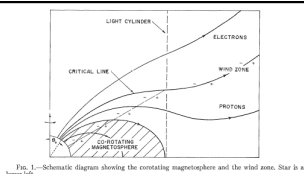


FIG. 1.—Schematic diagram showing the containing magnetosphere and the wind zone. Star is at lower left.

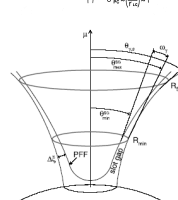
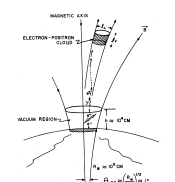
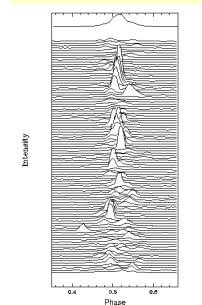
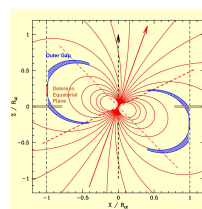


FIG. 1.—Schematic diagram showing the containing magnetosphere and the wind zone. Star is at lower left.



12 Sep '11

Course II: Compact Objects, the Dynamic Sky and 21st Century Radio Telescopes

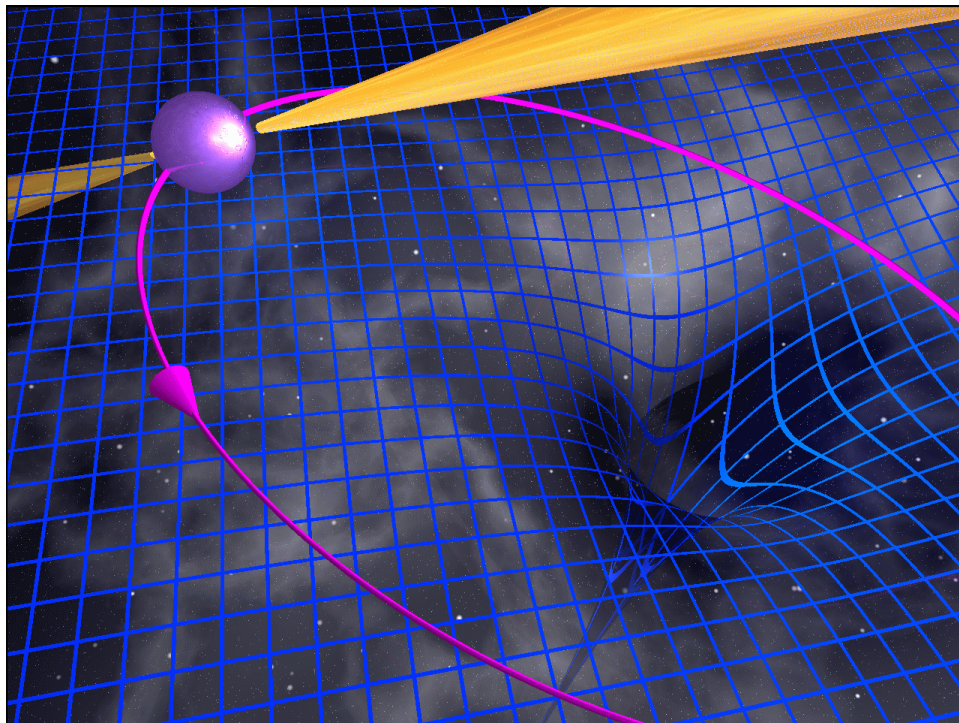
Binary Pulsars

- Most pulsars are isolated (not in binaries)
- Binary pulsars (about 1% of all pulsars):
 - White dwarf companions ($\sim 2/3$ of millisecond pulsars)
 - Neutron star companions
 - Black hole companions (should exist, none known)
- Other companions:
 - planets (2 to 3 pulsars) (Note: first extrasolar planets detected !)
 - debris disks (not seen directly but inferred)
- **Importance:** testing theories of gravity, including General Relativity, precision masses of NS

12 Sep '11

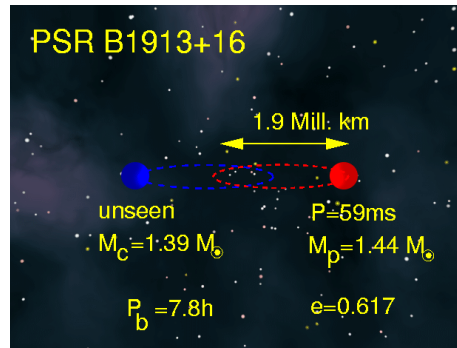
Course II: Compact Objects, the Dynamic Sky and 21st Century Radio Telescopes

9

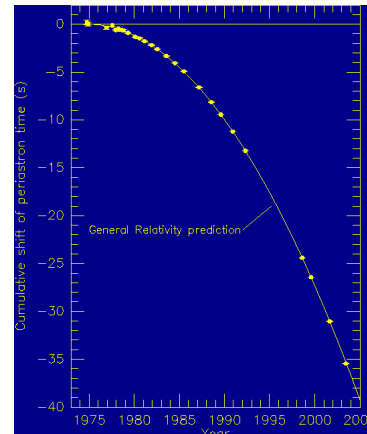


The Hulse-Taylor Binary Pulsar

Hulse & Taylor (1974)



Weisberg & Taylor (priv. comm)

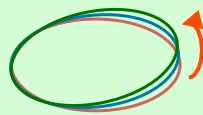


- Orbit shrinks every day by 1cm
- Confirmation of existence of gravitational waves

12 Sep '11

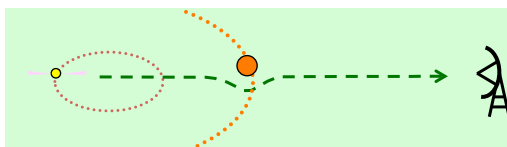
Course II: Compact Objects, the Dynamic Sky and 21st Century Radio Telescopes

11



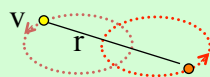
Precession

$$\dot{\omega} = 3 \left(\frac{P_b}{2\pi} \right)^{-5/3} \frac{1}{1-e^2} \left[\frac{G}{c^3} (m_1 + m_2) \right]^{2/3}$$



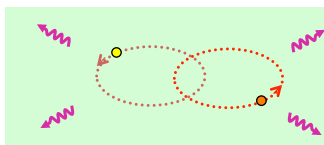
Shapiro Delay

$$\Delta t = 2 \frac{G}{c^3} m_2 \ln [1 - \sin i \sin(\varphi - \varphi_0)]$$



Grav Redshift/Time Dilation

$$\gamma = \frac{G^{3/2}}{c^2} \left(\frac{P_b}{2\pi} \right)^{1/3} e \frac{m_2(m_1 + 2m_2)}{(m_1 + m_2)^{5/2}}$$



Gravitational Radiation

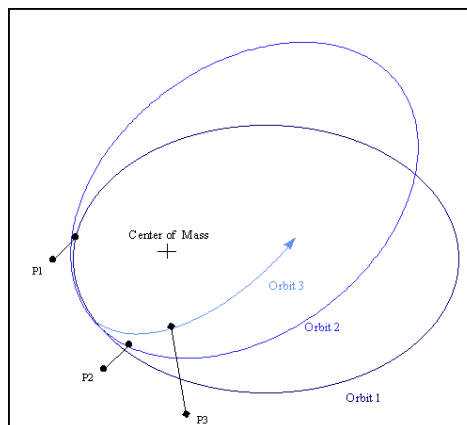
$$\dot{P}_b = - \left(\frac{192\pi}{5} \right) \frac{G^{5/2}}{c^5} \left(\frac{P_b}{2\pi} \right)^{-5/2} \left(1 + \frac{73}{24} e^2 + \frac{37}{96} e^4 \right) \frac{1}{(1-e^2)^{3/2}} \frac{m_1 m_2}{(m_1 + m_2)^{5/2}}$$

12 Sep '11

Course II: Compact

Precession of Orbits

- Precession of Mercury's orbit was known by Einstein to not be fully accounted for by perturbations from other planets in the solar system
- The unexplained part of Mercury's advance of perihelion (**43 arc sec/century**) was explained by Einstein, the first empirical triumph for GR.
- The periastron of PSR B1913+16 advances **4.2 degrees/year**. The daily periastron advance is the same as Mercury's perihelion advance in a century...
- The periastron advance of the double pulsar J0737-3039A,B is **16.9 degrees/year**

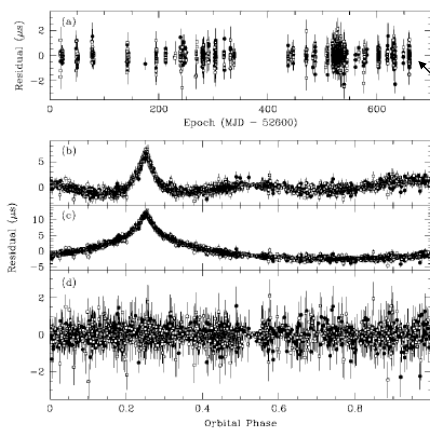


12 Sep '11

Course II: Compact Objects, the Dynamic Sky and 21st Century Radio Telescopes

13

One of the best pulsars for timing



MSP J1909-3744 $P=3$ ms + WD

Jacoby et al. (2005)

Weighted $\sigma_{\text{TOA}} = 74$ ns

Shapiro delay

FIG. 1.—High-precision timing residuals for PSR J1909-3744. Filled circles represent TOAs from the 1341 MHz band, while open squares denote the 1405 MHz band. (a) Residuals vs. observation epoch for best-fit model taking Shapiro delay fully into account (Table 1). (b) Residuals vs. orbital phase for best-fit Keplerian model. Some of the Shapiro delay signal is absorbed in an anomalously large Roemer delay and eccentricity. (c) Residuals vs. orbital phase for the best-fit model, but with the companion mass set to zero (i.e., the correct Keplerian orbit, but neglecting Shapiro delay). (d) Residuals vs. orbital phase for the best-fit model taking Shapiro delay fully into account (Table 1).

12 Sep '11

Course II: Compact Objects, the Dynamic Sky and 21st Century Radio Telescopes

14

A Double-Pulsar System: A Rare Laboratory for Relativistic Gravity and Plasma Physics

A. G. Lyne,^{1*} M. Burgay,² M. Kramer,¹ A. Possenti,^{3,4}
 R.N. Manchester,⁵ F. Camilo,⁶ M. A. McLaughlin,¹ D. R. Lorimer,¹
 N. D'Amico,^{3,7} B. C. Joshi,⁸ J. Reynolds,⁹ P. C. C. Freire¹⁰

The clocklike properties of pulsars moving in the gravitational fields of their unseen neutron-star companions have allowed unique tests of general relativity and provided evidence for gravitational radiation. We report here the detection of the 2.8-second pulsar J0737–3039B as the companion to the 23-millisecond pulsar J0737–3039A in a highly relativistic double neutron star system, allowing unprecedented tests of fundamental gravitational physics. We observed a short eclipse of J0737–3039A by J0737–3039B and orbital modulation of the flux density and the pulse shape of J0737–3039B, probably because of the influence of J0737–3039A's energy flux on its magnetosphere. These effects will allow us to probe magneto-ionic properties of a pulsar magnetosphere.

www.sciencemag.org SCIENCE VOL 303 20 FEBRUARY 2004

12 Sep '11

Course II: Compact Objects, the Dynamic Sky and 21st Century Radio Telescopes

15

Equations for Relativistic Orbits

Keplerian parameters:

Classical measurements of orbit give 5 parameters (P_b , x , e , ω , t_p) and the mass function. One additional GR measurement is needed to determine the masses M_1 and M_2 separately

$$f = \frac{(m_2 \sin i)^3}{M^2} = \left(\frac{2\pi}{P_b}\right)^2 x^3 T_\odot^{-1}$$

$$M = M_1 + M_2$$

$$x = a_1 \sin i / c$$

$$T_\odot = GM_\odot / c^3 = 4.925 \mu s$$

GR Effects on Orbit:

$$\dot{\omega} = 3 \left(\frac{P_b}{2\pi}\right)^{-5/3} (T_\odot M)^{2/3} (1 - e^2)^{-1}$$

Orbital precession rate

$$\dot{P}_b = -\frac{192\pi}{5} \left(\frac{P_b}{2\pi}\right)^{-5/3} \left(1 + \frac{73}{24}e^2 + \frac{37}{96}e^4\right) \times (1 - e^2)^{-7/2} T_\odot^{5/3} m_1 m_2 M^{-1/3},$$

Decay of orbital period (GW emission)

$$\gamma = e \left(\frac{P_b}{2\pi}\right)^{1/3} T_\odot^{2/3} M^{-4/3} m_2 (m_1 + 2m_2),$$

Red shift + 2nd order Doppler effect

$$r_s = T_\odot m_2,$$

r_s = Shapiro delay parameters

$$s = x \left(\frac{P_b}{2\pi}\right)^{-2/3} T_\odot^{-1/3} M^{2/3} m_2^{-1}.$$

12 Sep '11

Course II: Compact Objects, the Dynamic Sky and 21st Century Radio Telescopes

16

NS Masses

NS masses determined from Keplerian orbital elements + GR orbital effects (Shapiro delay, orbital decay)

Millisecond pulsars accrete $\sim 0.1 M_{\odot}$ more mass than NS-NS binaries that accrete for shorter times

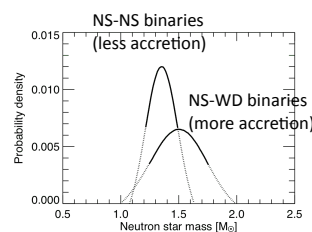
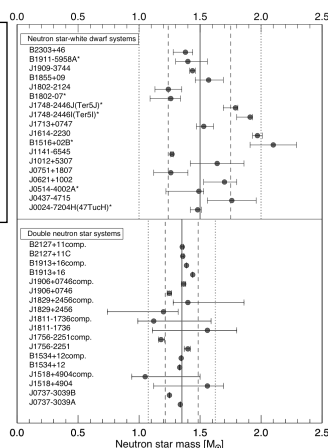


Figure 2. Posterior predictive density estimates for the neutron star mass distribution. DNS and NS-WD systems have respective peaks at $1.35 M_{\odot}$ and $1.50 M_{\odot}$. Probability densities are normalized to show the 95% posterior probability range. The solid parts of the curves show the central 68% probability range which correspond to $1.35 \pm 0.13 M_{\odot}$ and $1.50 \pm 0.23 M_{\odot}$ for the DNS and NS-WD system, respectively.







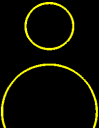
Kiziltan et al. 2010

12 Sep '11

Course II: Compact Objects, the Dynamic Sky and 21st Century Radio Telescopes

19

Double Neutron Star Binaries

	P_{orb}	e	
	2.46 hr	0.09	J0737-3039A
	3.98 hr	0.09	J1906+0746
	7.67 hr	0.18	J1756-2251
	7.75 hr	0.62	B1913+16
	8.05 hr	0.68	B2127+11C
	10.10 hr	0.27	B1534+12
	28.22 hr	0.14	J1829+2456

Nine known NS-NS binaries

These objects will merge in ~ 100 Myr

Mergers produce:

- Gamma-ray bursts
- Chirped gravitational wave signature
- Particle blast waves

12 Sep '11

Course II: Compact Objects, the Dynamic Sky and 21st Century Radio Telescopes

20



22

Radio Emission from Pulsars

- Totally unexpected
- Radio emission is weak (for most pulsars) in terms of detectability
- But given the size of the neutron star and its magnetosphere, it is remarkable that we can detect them at all.
- Why can such small volumes produce detectable radiation?
- Answer: radio emission is coherent (from plasma bunching or plasma maser)
 - two-stream instability
 - langmuir collapse, solitons

N = number of particles
 Intensity $\sim N^2$ coherent
 $\sim N$ incoherent

12 Sep '11

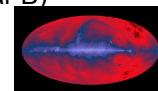
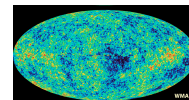
Course II: Compact Objects, the Dynamic Sky and 21st Century Radio Telescopes

23

Kinds of Astrophysical Radio Emission

Continuum:

- | | | |
|------------|---|---|
| incoherent | { | – Thermal emission from ionized gas (bremsstrahlung, free-free emission); blackbody radiation |
| coherent | | – Synchrotron radiation (e^- spiraling in interstellar B) |
| | { | – Solar bursts: swept-frequency, narrowband radiation |
| | | – Pulsar radiation |



Spectral line:

- | | | |
|------------|---|---|
| incoherent | { | – Recombination lines (H, He, C) |
| coherent | | – 21 cm hyperfine emission from H |
| | { | – Molecular maser emission (OH, H ₂ O, methanol, SiO...) |
| | | |

12 Sep '11

Course II: Compact Objects, the Dynamic Sky and 21st Century Radio Telescopes

24

Coherent Astrophysical Signals

- Most radiation produced by astrophysical sources is *temporally incoherent* and *partly spatially coherent*:
 - blackbody radiation from stars: temporally incoherent, but compact (partial coherence)
 - cosmic microwave background: temporally incoherent and spatially incoherent (isotropic)
 - masers (microwave amplification by stimulated emission of radiation): temporally incoherent, high spatial coherence
 - pulsars: very high spatial coherence, sometimes highly temporally coherent

12 Sep '11

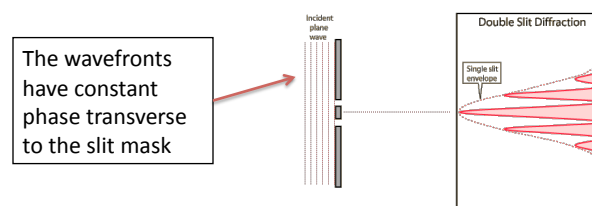
Course II: Compact Objects, the Dynamic Sky and 21st Century Radio Telescopes

25

Spatial Coherence

Coherent radiation has all of its sinusoidal components *in phase*

- Spatial coherence: two-slit diffraction pattern



- Spatial coherence is required to see the pattern of constructive and destructive interference in the diffraction pattern
- Spatial coherence is connected to the source size and to how different components of a source radiate

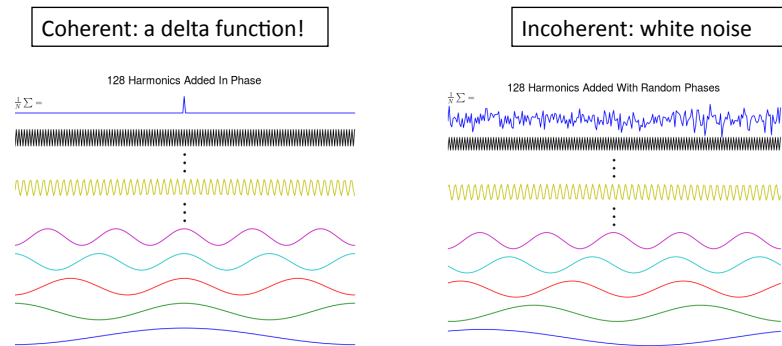
12 Sep '11

Course II: Compact Objects, the Dynamic Sky and 21st Century Radio Telescopes

26

Temporal Coherence

- Temporal coherence: describes the relationship of different Fourier components that make up a signal vs. time:



12 Sep '11

Course II: Compact Objects, the Dynamic Sky and 21st Century Radio Telescopes

27

Radiation Temperatures

- The radiation temperature of incoherent processes is limited by the mean particle energy:
 - Thermal: $kT_b < kT_{\text{particles}}$
 - Non-thermal: $kT_b < \langle \gamma mc^2 \rangle$ $\gamma = \text{Lorentz factor}$
- Incoherent synchrotron radiation: T_b is limited by inverse Compton radiation (ICR) to $\sim 10^{12}$ K because larger energies per particle cool rapidly from ICR.
- Coherent processes: the radiation temperature is essentially unbounded

12 Sep '11

Course II: Compact Objects, the Dynamic Sky and 21st Century Radio Telescopes

28

Radiation Temperatures

Rayleigh Jeans regime for blackbody radiation:

$$I_\nu = \frac{2h\nu^3}{c^2} \frac{1}{1 - e^{-h\nu/kT}} \approx \frac{2kT}{\lambda^2}$$

Flux density:

$$F_\nu = \int d\Omega I_\nu(\Omega) \approx \Omega_s I_\nu(max)$$

Time variable source:

$$l_s \sim c\Delta t \Rightarrow T_{\text{eff}} \sim \frac{\lambda^2 F_\nu}{2k} \left(\frac{D}{c\Delta t} \right)^2$$

$$\Omega_s \sim \left(\frac{c\Delta t}{D} \right)^2 \approx 3.5 \times 10^{17} \text{ K } F_\nu(\text{Jy}) \left(\frac{D_{\text{kpc}}}{\nu_{\text{GHz}} \Delta t_s} \right)^2$$

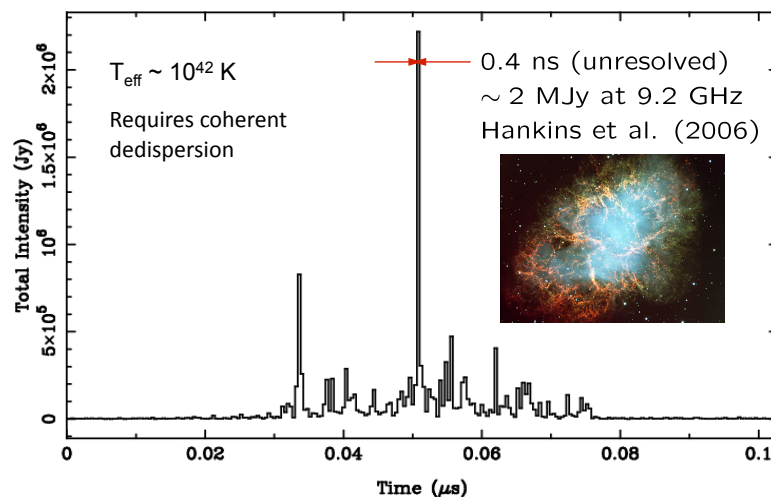
Unit of flux density: 1 Jansky = $10^{-23} \text{ erg s}^{-1} \text{ cm}^{-2} \text{ Hz}^{-1} = 10^{-26} \text{ watts m}^{-2} \text{ Hz}^{-1}$

12 Sep '11

Course II: Compact Objects, the Dynamic Sky and 21st Century Radio Telescopes

29

Nanoshots from the Crab Pulsar



12 Sep '11

Course II: Compact Objects, the Dynamic Sky and 21st Century Radio Telescopes

30

How do we “measure” Brightness Temperatures from Pulsars?

- We don't because we cannot measure the angular size of an emission region (too small)
- We can infer their size as follows:
 - For a source of size $2R$, the minimum duration of its emission is $\Delta t = 2R/c$ with c = speed of light.
 - We can estimate its angular size as $\theta_s = 2R/D$ where D = distance

- The brightness temperature is then

$$T_b = \frac{\lambda^2 S}{2k\Omega_s} \approx \frac{S}{2k} \left(\frac{D}{\nu \Delta t} \right)^2 \approx 10^{20.5} \text{ K} S_{\text{mJy}} \left(\frac{D_{\text{kpc}}}{\nu_{\text{GHz}} \Delta t_{\text{ms}}} \right)^2$$

12 Sep '11

Course II: Compact Objects, the Dynamic Sky and 21st Century Radio Telescopes

31

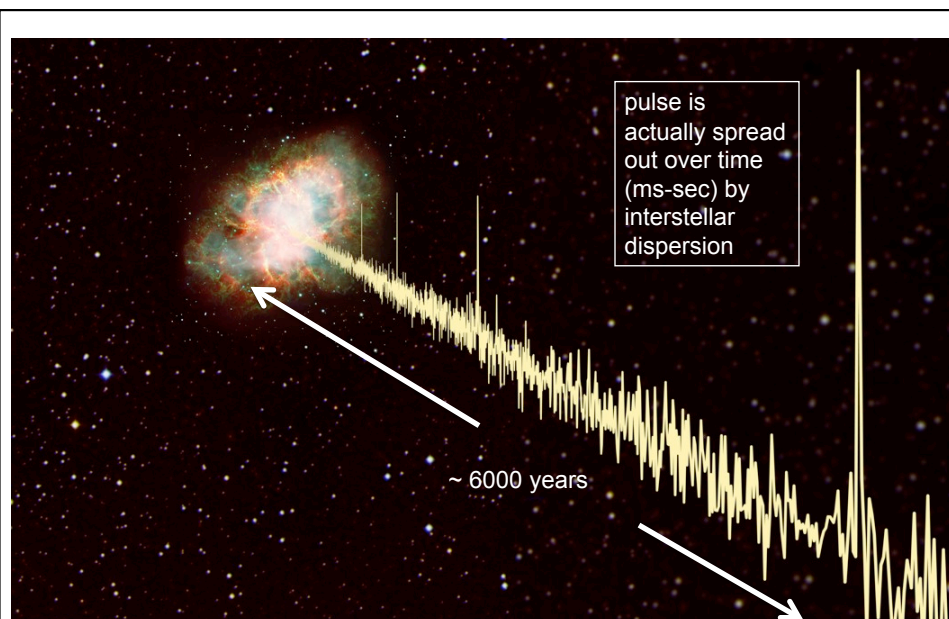


Image courtesy of NRAO/AUI and Joeri van Leeuwen (UC Berkeley) / ESO / AURA

12 Sep '11

Course II: Compact Objects, the Dynamic Sky and 21st Century Radio Telescopes

32

Plasma Propagation Effects

- Radio propagation phenomena (many)
- Dedispersion methods
- Kolmogorov-like microstructure in the ionized ISM
- Astronomical impacts:
 - Pulsar surveys
 - Precision pulsar timing to detect gravitational waves
 - Pulsars orbiting Sgr A* (GR tests, dark matter)
 - Scattering in the intergalactic medium

10 Dec 2010

NYU

33

Starting Point: Index of Refraction

- Dispersion relation in free space:
 - $\omega = kc$
 - phase velocity = group velocity = $\omega/k = c$
- Cold plasma (collisions not important):
 - No magnetic field:
 - $\omega = kc/n_r(\omega)$ $n_r(\omega) = (1 - \omega_p^2/\omega^2)^{1/2}$
 - $\omega_p^2 = \text{plasma frequency} = \frac{4\pi n_e e^2}{m}$
 - phase velocity = $c/n_r(\omega) > c$ (speed of phase fronts)
 - group velocity = $d\omega/dk = cn_r(\omega) < c$ (speed of a wave packet)
 - With magnetic field: birefringent (left, right)
 - $$n_{l,r} \approx 1 - \omega_p^2/2\omega^2 \mp \omega_p^2 \omega_{B\parallel}/2\omega^3$$
 - cyclotron frequency $\omega_{B\parallel} = \frac{eB \cos \theta}{m_e c}$

9/13/11

Course II: Compact Objects, the Dynamic Sky and 21st Century Radio Telescopes

34

Propagation through the interstellar plasma

Refractive indices for cold, magnetized plasma

$$n_{\ell,r} \sim 1 - \nu_p^2/2\nu^2 \mp \nu_p^2\nu_{B\parallel}/2\nu^3$$

$$\nu \gg \nu_p \sim 2 \text{ kHz} \quad \nu \gg \nu_{B\parallel} \sim 3 \text{ Hz}$$

Propagation velocities are frequency dependent:

Phase velocity: $v_p = \frac{\omega}{k} = \frac{c}{n_{\ell,r}}$

Group velocity: $v_g = \frac{\partial \omega}{\partial k} = \frac{\partial}{\partial k} \left(\frac{kc}{n_{\ell,r}} \right)$

Group delay = $\Delta(\text{Time of Arrival})$

$$t = t_{\text{DM}} \pm t_{\text{RM}}$$

$$t_{\text{DM}} = 4.15 \text{ ms DM } \nu^{-2}$$

$$t_{\text{RM}} = 0.18 \text{ ns RM } \nu^{-3}$$

birefringence



Dispersion Measure DM = $\int ds n_e$ units: pc cm⁻³

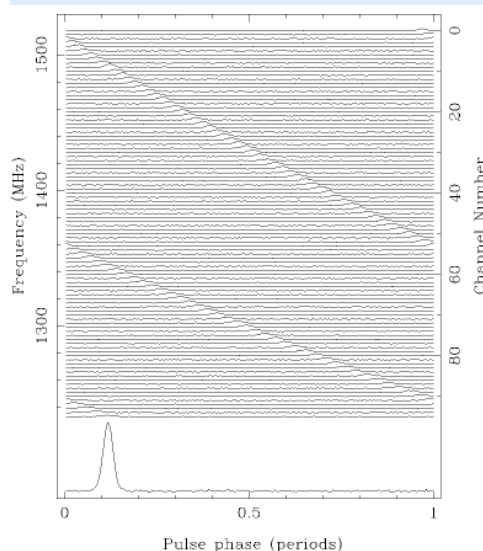
Rotation Measure RM = $0.81 \int ds n_e B_{\parallel}$ units: rad m⁻²

10 Dec 2010

NYU

35

Dispersion



$$t_{\text{DM}}(\nu) = \frac{4.15 \times \text{DM ms}}{\nu_{\text{GHz}}^2}$$

High frequencies arrive earlier than low frequencies

DM is unique to each pulsar

DM changes with time due to motion of the pulsar and turbulence in the interstellar medium

9/13/11

Course II: Compact Objects, the Dynamic Sky and 21st Century Radio Telescopes

36

Dedispersion

Two methods:

Coherent:

- operates on the voltage proportional to the electric field accepted by the antenna, feed and receiver
- computationally intensive because it requires sampling at the rate of the total bandwidth
- “exact”

Post-detection:

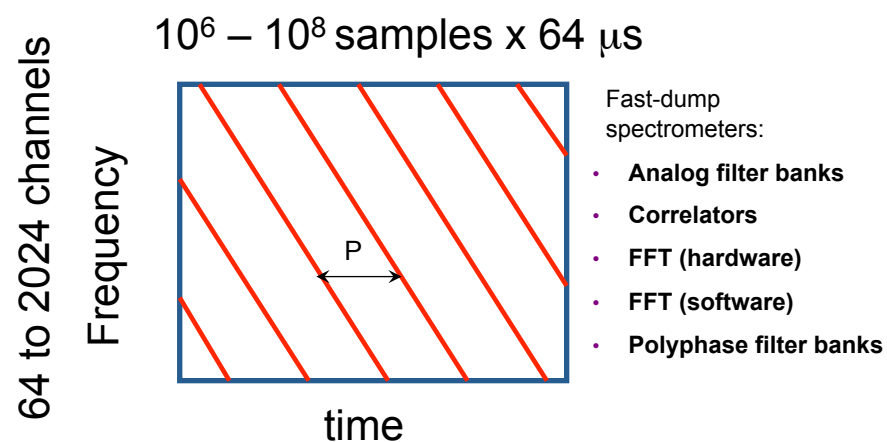
- operates on intensity = $|\text{voltage}|^2$
- computationally less demanding
- an approximation

9 June 2011

IPTA Morgantown

37

Basic data unit = a dynamic spectrum



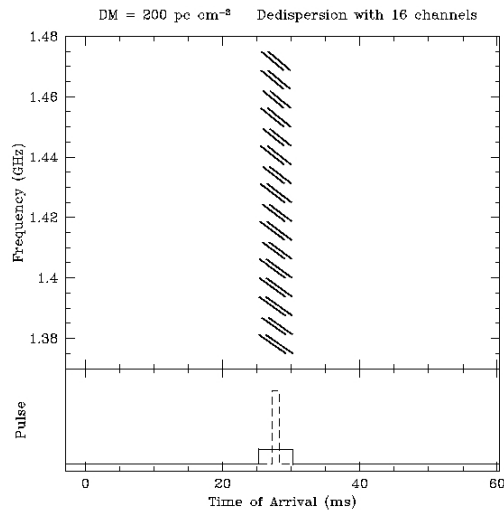
9 June 2011

IPTA Morgantown

38

Post-detection Dedispersion:

Sum intensity over frequency after correcting for dispersion delay



Residual time smearing:

$$\Delta t = [\Delta t_{DM}^2 + (1/\Delta \nu)^2]^{1/2}$$

$$= [(a\Delta \nu)^2 + (\Delta \nu)^{-2}]^{-1/2}$$

\Rightarrow minimum smearing time across a channel when

$$\Delta \nu = [8.3 \mu s DM \nu^{-3}]^{-1/2}$$

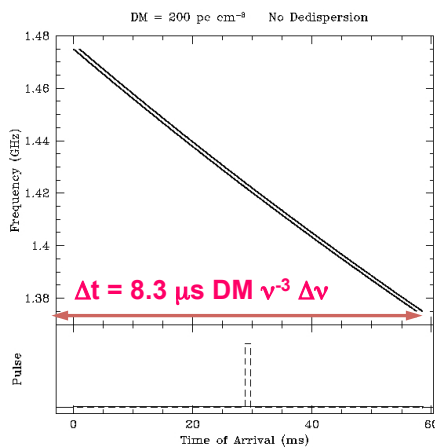
A consequence of the uncertainty principle for Fourier transforms:
 $\Delta \nu \Delta t \sim 1$

9 June 2011

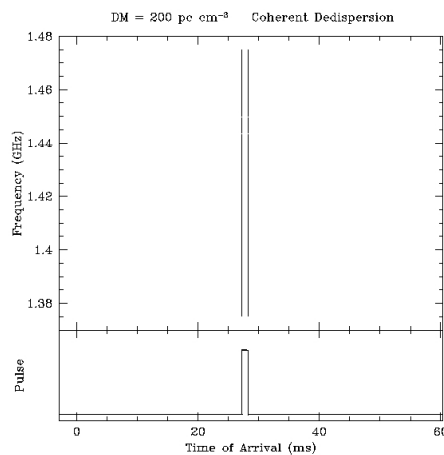
IPTA Morgantown

39

Dispersed Pulse



Coherently dedispersed pulse



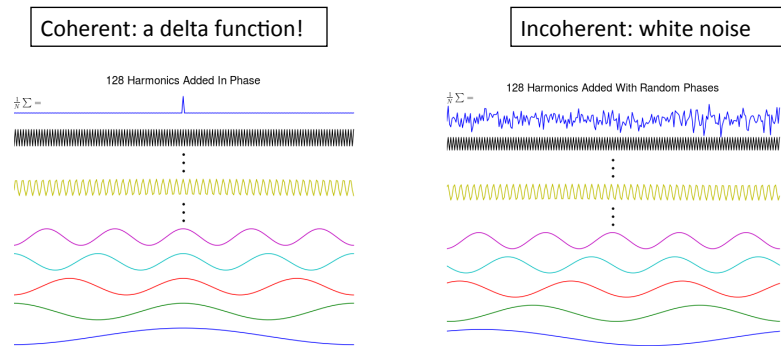
9 June 2011

IPTA Morgantown

40

Temporal Coherence

- Temporal coherence: describes the relationship of different Fourier components that make up a signal vs. time:



12 Sep '11

Course II: Compact Objects, the Dynamic Sky and 21st Century Radio Telescopes

41

Coherent Dedispersion

pioneered by Tim Hankins (1971)

Dispersion delays in the time domain represent a phase perturbation of the electric field in the Fourier domain:

$$\vec{E}_{\text{measured}}(\omega) = \vec{E}_{\text{emitted}}(\omega) e^{ik(\omega)z}$$

Coherent dedispersion involves multiplication of Fourier amplitudes by the inverse function,

$$e^{-ik(\omega)z}$$

An
example
of
matched
filtering

For the non-uniform ISM, we have

$$k(\omega)z \rightarrow \int dz k(\omega) \propto \omega^2 \text{DM} + \text{constant}$$

which is known to high precision for known pulsars.

The algorithm consists of

$$\text{IFFT}\{\text{FFT}[E_{\text{measured}}(t)] \times e^{-ik(\omega)z}\} \approx E_{\text{emitted}}(t)$$

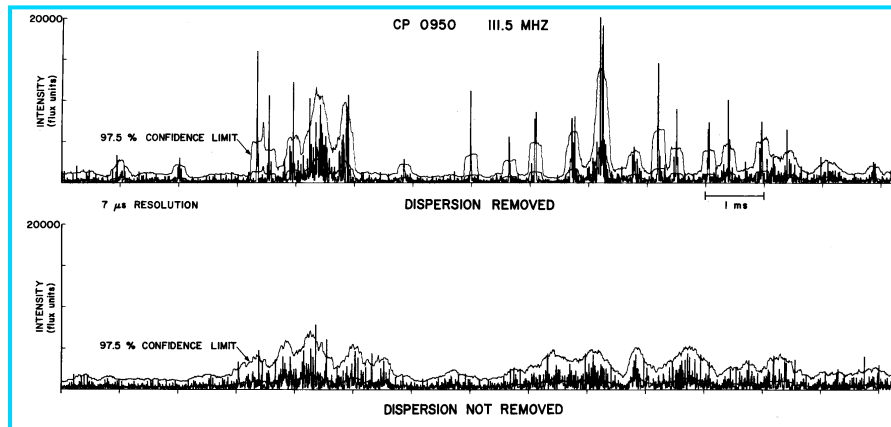
Application requires very fast sampling to achieve usable bandwidths.

One
parameter:
DM

10 July 2007

Single Dish Summer School 2007

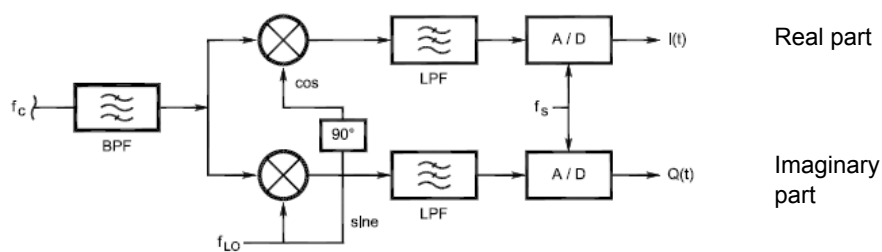
Micropulses coherently dedispersed (Hankins1971)



10 July 2007

Single Dish Summer School 2007

Backend stage of mixing: quadrature baseband mixing



$$\epsilon(t) = I(t) + iQ(t) = \text{complex baseband signal}$$

voltage at intermediate frequency in heterodyned system:

$$v(t) = \text{Re} \{ \epsilon(t) e^{2\pi i f_0 t} \} = \text{real}$$

9/16/09

A6520

44

Coherent Dedispersion

pioneered by Tim Hankins (1971)

Coherent dedispersion works by explicit deconvolution:

$$E_{\text{measured}}(t) = E_{\text{emitted}}(t) * \text{FFT}\{e^{ik(\omega)z}\}$$

$$\Rightarrow E_{\text{emitted}}(t) \approx E_{\text{measured}}(t) * \text{FFT}\{e^{-ik(\omega)z}\}$$

Comments and Caveats:

- Software implementation with FFTs to accomplish deconvolution (Hankins 1971)
- Hardware implementations: real-time FIR filters (e.g. Backer et al. 1990s-present)
- Resulting time resolution: $1 / (\text{total bandwidth})$
- Requires sampling at Nyquist rate of 2 samples \times bandwidth
 \Rightarrow Computationally demanding
- Actual time resolution often determined by interstellar scattering (multipath)
- **Most useful for low-DM pulsars and/or high-frequency observations**

10 July 2007

Single Dish Summer School 2007

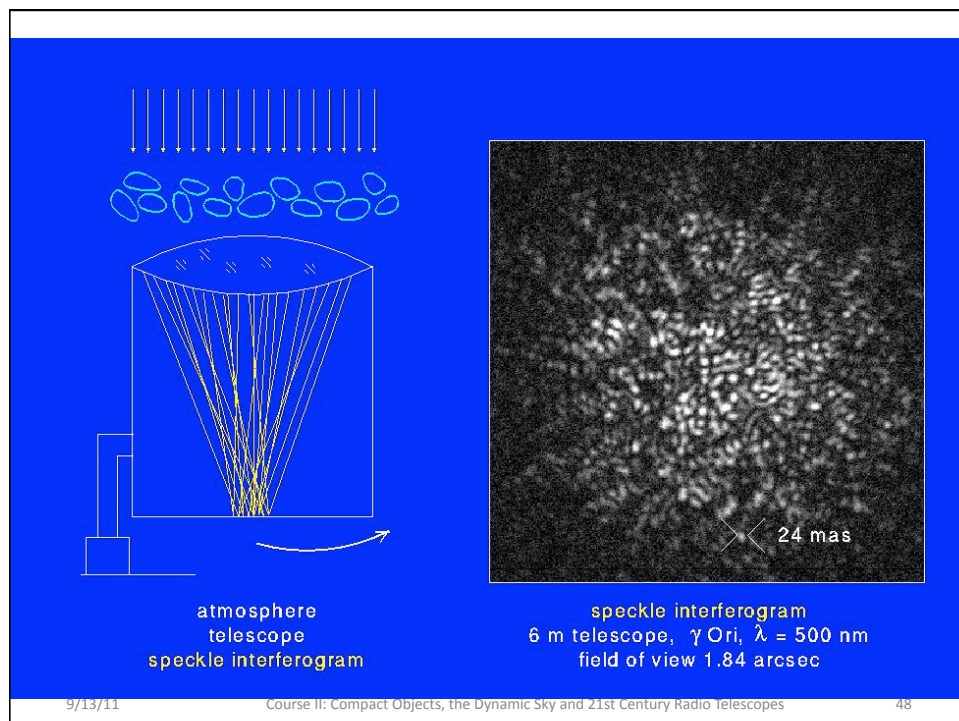
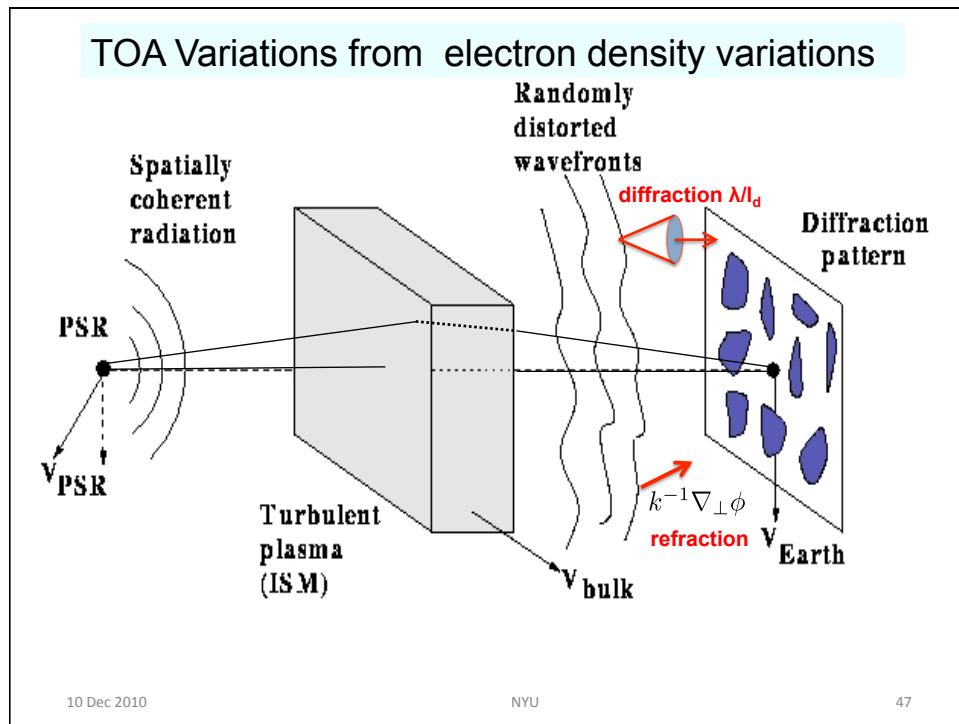
Interstellar Radio Scattering

- Discovered as angular broadening (“seeing”) of interstellar OH masers (1.6 GHz) (1967)
- Also discovered as scintillations (“twinkling”) of pulsar intensities (1968)
- Both are diffraction effects:
 - Angular: $\theta_d \approx \lambda / l \approx 1 \text{ mas}$ for $l \approx 10^4 \text{ km}$
 - Temporal broadening: $\tau_d \sim D\theta_d^2 / 2c \sim 1 \text{ ms}$ for $D = 1 \text{ kpc}$
 - Correlation bandwidth for scintillations $\sim 1 / \tau_d$
- Why pulsars are especially useful:
 - Require source size $\leq \lambda / D\theta_d \sim 1 \mu\text{as}$ to see twinkling (the “stars twinkle, planets do not” effect)
 - Much smaller than an active galactic nucleus
 - Pulsar magnetosphere: $\theta \sim cP/2\pi D \sim 0.1\mu\text{as}$
 - Pulsars emit coherent radio emission (AGNs: incoherent)

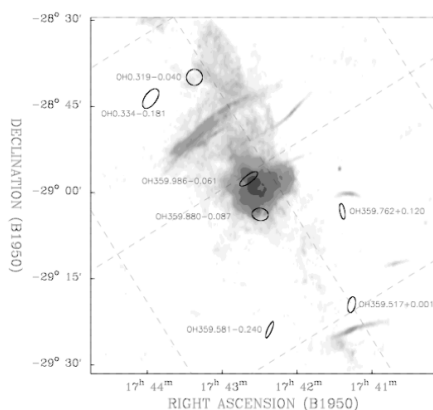
10 Dec 2010

NYU

46

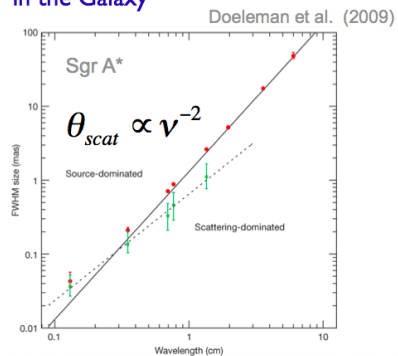


Scattering of Sgr A* and GC Pulsars



Frail et al. (1994)

- Temporal and angular broadening by turbulent ionized gas
- The most scattered line of sight in the Galaxy



10 Dec 2010

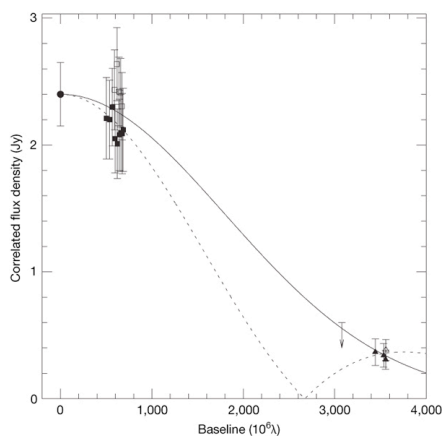
NYU

49

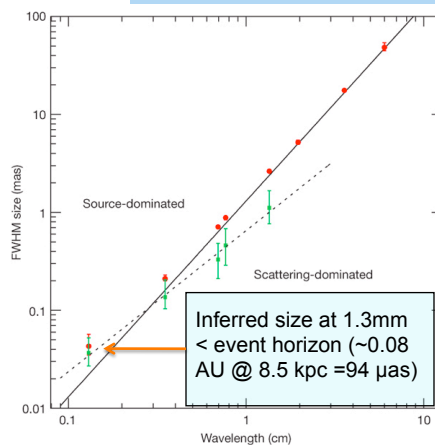
Size of Sgr A* ($4 \times 10^6 M_{\odot}$)

Doeleman et al. 2008

Visibility Function at 1.3mm



Angular size vs λ



9/13/11

Course II: Compact Objects, the Dynamic Sky and 21st Century Radio Telescopes

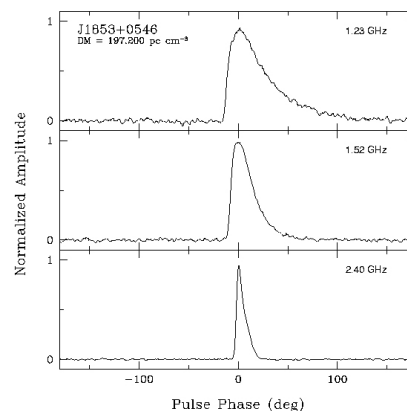
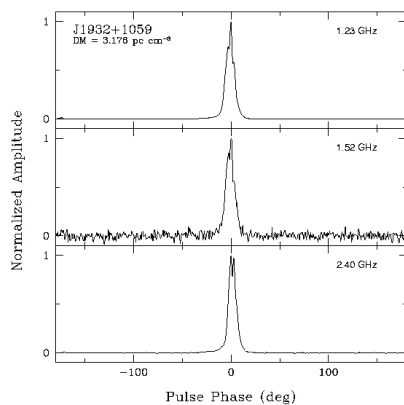
50

Pulse broadening from interstellar scattering:

$$\tau_d \sim \frac{\text{rms excess path length}}{c} \sim \frac{D\theta_d^2}{2c} \propto \nu^{-4}$$

Low-DM pulsar: $\tau_d \ll$ pulse width

High-DM pulsar: $\tau_d \sim$ pulse width

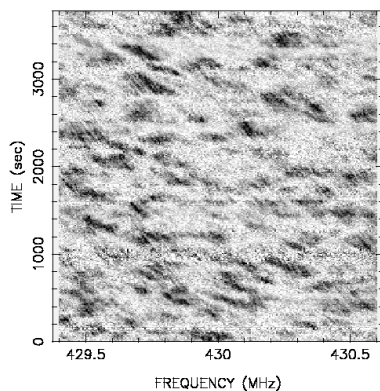


Arecibo WAPP data, Bhat et al 2004

10 July 2007

Single Dish Summer School 2007

PSR 1737+13 0.430 GHz MJD 44830 2251117

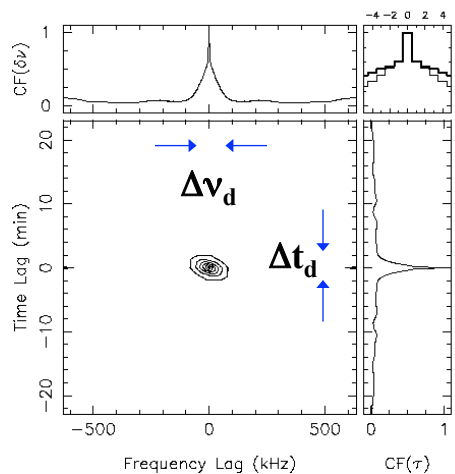


2D Autocorrelation Function
 \Rightarrow Characteristic DISS frequency
 and time scales

10 Dec 2010

Dynamic Spectrum Diffractive Interstellar Scintillations

PSR 1737+13 0.430 GHz MJD 44830 2251117



NYU

52

Turbulence in Ionized ISM

- Extends to scales ~ 100 -1000 km
- Similar to Kolmogorov turbulence in a neutral, incompressible fluid
 - ISM is ionized
 - ISM is compressible
 - no worries: the electron density is a “passive tracer” of the true turbulence in the velocity field and magnetic field in the ISM
 - the turbulence appears to be anisotropic: small scale fluctuations are oriented relative to the interstellar magnetic field

10 Dec 2010

NYU

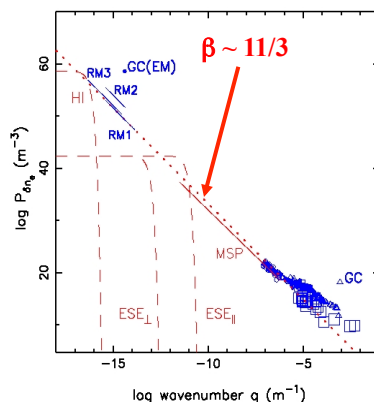
53

Estimated Wavenumber Spectrum for δn_e

$$\text{Spectrum} = C_n^2 q^{-\beta}$$

$$\langle n_e^2 \rangle = \int d^3 q C_n^2 q^{-\beta}$$

$$\text{SM} = \int_{\text{LOS}} ds C_n^2(s)$$



Constraints on spectrum:

Small scales: (100s km to 1000 AU)

- Scaling of DISS parameters with v
 - angle, frequency, time
- Scintillation arcs
- DM(t) on months to years
- DM(θ) in globular clusters
- RISS parameters

Large scales: (0.01 pc to 100 pc)

- RM vs $\delta\theta$
- EM, DM, SM on same LOS
- Bow shock contours (Guitar Neb)

All scales:

- Cosmic ray scattering on δB and linkage $\delta n_e/n_e \sim \delta B/B$

Anisotropies seen on heavily scattered LOS: connection to B

see also Armstrong, Rickett, Spangler 1995

10 Dec 2010

NYU

54